# Phonons in a magnetized Coulomb crystal of ions with polarizable electron background

D. A. Baiko[a] and A. A. Kozhberov
*Ioffe Institute, Politekhnicheskaya 26, Saint Petersburg 194021, Russian Federation*

(Received 28 July 2017; accepted 8 October 2017; published online 7 November 2017)

We have studied phonon modes of a body-centered cubic (bcc) Coulomb crystal of ions in the presence of a uniform magnetic field B taking into account the polarizability of the electron background (electron screening) described by the Thomas-Fermi formalism. For $k \gg \kappa_{\rm TF}$ (k and $\kappa_{\rm TF}$ are the phonon wavevector and Thomas-Fermi wavenumber, respectively), electron polarizability is not important. At $k \ll \kappa_{\rm TF}$, the electron response results in a pronounced effect. One of the three available modes is acoustic. For orthogonal propagation ($\mathbf{k}\perp\mathbf{B}$), its frequency $\Omega$ is independent of $B$ and $\kappa_{\rm TF}$. For $\mathbf{k} \parallel \mathbf{B}$, $\Omega \propto 1/\kappa_{\rm TF}$ and is independent of $B$. Another mode is quadratic. Its frequency is $\propto 1/(B\kappa_{\rm TF})$ for orthogonal propagation and $\propto 1/B$ and independent of $\kappa_{\rm TF}$ for the parallel case. The third mode is optic with $\Omega \approx \omega_{\rm B}$ ($\omega_{\rm B}$ is the ion cyclotron frequency). A general expression is derived for the dynamic matrix of a Coulomb crystal with a polarizable background and more than one ion in the primitive cell. It is employed for a study of a magnetized hexagonal close-packed Coulomb crystal. We have also presented an analysis of phonon polarization vectors in a magnetized bcc crystal with or without screening. The results obtained can be used for realistic calculations of electron-phonon scattering rates and electron thermal and electrical conductivities in neutron star crusts. *Published by AIP Publishing*. https://doi.org/10.1063/1.4998008

## I. INTRODUCTION

A Coulomb crystal is a system of point charges arranged in a perfect lattice and immersed into a constant and uniform background of opposite charge. The main difference between Coulomb crystals and ordinary terrestrial crystals is that in the former, the charges at the lattice nodes interact via a pure long-range Coulomb force. For an adequate description of such a system, interactions of a given charge with all the other charges in the lattice have to be taken into account.

Large-scale Coulomb crystals are anticipated to form in inner layers of white dwarfs and in crusts of neutron stars. In both cases, there are atoms which are compressed by gravity to very high densities, which results in complete pressure-ionization by strongly degenerate electrons. If the temperature is sufficiently low, numerical simulations[1] and certain observations[2] indicate that the ions arrange themselves in a lattice. It is typically assumed that the body-centered cubic (bcc) lattice forms in these compact astrophysical objects as it is known to be thermodynamically preferable to other lattices for a pure Coulomb interaction.

The phonon properties of Coulomb crystals are of crucial importance for white dwarf and neutron star physics. In a wide range of densities and temperatures, phonons determine the specific heat of matter in these stars and thus their cooling and evolution of their surface temperature. Besides that, electron-phonon scattering is a dominant mechanism limiting electron thermal and electrical conductivities and shear viscosity. Thermal conductivity determines the rate at which heat is transported from the hot inner layers to the surface of these stars. Electrical conductivity is required for studies of magnetic field diffusion and drift. Shear viscosity sets the timescale for attenuation of various potentially observable seismic modes.

Coulomb crystal phonons have been studied in a great number of works of which the most relevant for our purposes are those of Cohen and Keffer[3] and Carr,[4] who had studied the dynamic matrix, frequencies, and polarization vectors of the modes of an ideal Coulomb crystal (with a rigid electron background); Pollock and Hansen,[5] who had included the effect of electron screening or finite polarizability (or compressibility) of the electron background; and Usov *et al.*,[6] who had initiated studies of Coulomb crystals in magnetic fields. More recent developments were partially summarized in Ref. 7.

It has been shown[8] that modification of Coulomb crystal phonons in a magnetic field (phonon magnetization) has a profound effect on electron-phonon scattering rates and thermal and electrical conductivities. In that work, quantization of electron motion in a strong magnetic field was not taken into account, but the trend appeared to be such that an even stronger effect could be anticipated if electrons populated only the ground Landau level. In order to check this hypothesis, one would have to perform new calculation of electron-phonon scattering with a proper electron distribution function in a magnetic field. However, if electrons are restricted to the ground Landau level, they lose kinetic energy with a decrease in density very quickly. Hence, they rapidly become polarizable, and in order for the new calculations to be self-consistent, one should include electron gas compressibility into a description of crystal phonons. Unfortunately, phonons in a magnetized Coulomb crystal with a polarizable electron background have not been previously considered.

[a]Electronic mail: baiko@astro.ioffe.ru

In this paper, we intend to fill this void and present an analysis of phonons in an ion Coulomb crystal with effects of electron screening and magnetization of the ion motion taken into account simultaneously.

## II. GENERAL FORMALISM

In order to describe lattice phonons, one has to treat ion motion microscopically. Since the ions move slowly, their current can be neglected, and the electric field is determined by the instantaneous charge density. The scalar potential is sufficient to describe this system, and the electric field is purely longitudinal.

Polarization of the electron background can be described by the dielectric function formalism. It results in a modification of the electron density in response to the ion presence. For the same reason, we can treat this adjustment as instantaneous. Accordingly, we only need to know the static longitudinal dielectric function of electrons $\epsilon(\mathbf{k}) \equiv \tilde{\epsilon}_{\mu\nu}(\omega=0,\mathbf{k})k_\mu k_\nu/k^2$ (Greek indices denote Cartesian coordinates, summation over repeated Greek indices is implied, $\omega$ is the frequency, $\mathbf{k}$ is the wavevector, and $\tilde{\epsilon}_{\mu\nu}$ is the full dielectric tensor).

The dielectric function of a degenerate magnetized relativistic electron gas was studied by many authors starting from the work of Svetozarova and Tsytovich[9] based on the random-phase approximation. The general formulae are rather cumbersome, and we will restrict ourselves to the long-wavelength limit, where it reduces[10,11] to the Thomas-Fermi form $\epsilon(\mathbf{k}) = 1 + \kappa_{\rm TF}^2/k^2$, with $\kappa_{\rm TF}^2 = 4\pi e^2 \partial n_e/\partial\mu_e$. In the presence of the magnetic field $\mathbf{B}$

$$\kappa_{\rm TF}^2 = \frac{e^2|e|B}{\pi}\int_{-\infty}^{+\infty} \mathrm{d}p_\parallel \sum_{L=0}^{\infty}(2-\delta_{L,0})\left(-\frac{\partial f}{\partial\varepsilon}\right). \tag{1}$$

In this case, $e$, $n_e$, and $\mu_e$ are the electron charge, number density, and chemical potential, respectively, $p_\parallel$ is the electron momentum along the magnetic field, $\varepsilon = \sqrt{m_e^2 + p_\parallel^2 + 2|e|BL}$ and $m_e$ are the electron energy and mass, respectively, $L$ is the Landau level number, and $f$ is the Fermi-Dirac distribution function.

If $\mathbf{r}_I = \mathbf{R}_I + \mathbf{u}_I$ is the exact position of the $I$th ion ($\mathbf{R}_I$ and $\mathbf{u}_I$ being the $I$th lattice node and the ion displacement from it), the following equation of motion can be written in the absence of electron screening and external magnetic field:

$$\begin{aligned} m\ddot{\mathbf{u}}_I &= Z^2e^2\left[\sum_{J\neq I}\frac{\mathbf{r}_I-\mathbf{r}_J}{|\mathbf{r}_I-\mathbf{r}_J|^3} - n\int\frac{\mathrm{d}\mathbf{r}\,(\mathbf{r}_I-\mathbf{r})}{|\mathbf{r}_I-\mathbf{r}|^3}\right] \\ &= -\frac{\partial}{\partial\mathbf{r}_I}\int\frac{\mathrm{d}\mathbf{q}}{(2\pi)^3}\frac{4\pi Z^2e^2}{q^2} \\ &\quad\times\left[\sum_{J\neq I} e^{i\mathbf{q}\cdot(\mathbf{r}_I-\mathbf{r}_J)} - n\int\mathrm{d}\mathbf{r}\,e^{i\mathbf{q}\cdot(\mathbf{r}_I-\mathbf{r})}\right]. \end{aligned} \tag{2}$$

In this case, $n = n_e/Z$ is the ion number density, $m$ and $Z$ are the ion mass and charge number, respectively, and $\mathbf{q}$ is the integration variable in the wavevector space.

On the right-hand side, we have $Z|e|$ times the electric field at $\mathbf{r}_I$ created by the "unperturbed" charge density $\rho_{\rm ext}$ (i.e., all ions plus uniform electron background) with the $I$th ion excluded. If electron polarization is turned on,[11,12] the total charge density in momentum space ("unperturbed" plus polarization contributions) is $\rho(\mathbf{q}) = \rho_{\rm ext}(\mathbf{q})/\epsilon(\mathbf{q})$. However, the polarization contribution due to the $I$th ion exerts no force on the ion itself. Consequently, we obtain

$$\begin{aligned} m\ddot{\mathbf{u}}_I = &-\int\frac{\mathrm{d}\mathbf{q}}{(2\pi)^3}\frac{4\pi Z^2e^2}{q^2\epsilon(\mathbf{q})}i\mathbf{q} \\ &\times\left[\sum_{J\neq I} e^{i\mathbf{q}\cdot(\mathbf{r}_I-\mathbf{r}_J)} - n\int\mathrm{d}\mathbf{r}\,e^{i\mathbf{q}\cdot(\mathbf{r}_I-\mathbf{r})}\right]. \end{aligned} \tag{3}$$

At this point, we can drop the electron background term which is clearly equal to zero. The next step is to assume that the ion displacements $\mathbf{u}$ are much smaller than the separation between any two lattice nodes and expand the right-hand side of Eq. (3) in powers of the former. The zero-order terms vanish, and we obtain

$$\begin{aligned} m\ddot{\mathbf{u}}_I = &-\int\frac{\mathrm{d}\mathbf{q}}{(2\pi)^3}\frac{4\pi Z^2e^2}{q^2\epsilon(\mathbf{q})}i\mathbf{q} \\ &\times\sum_{J\neq I} i\mathbf{q}\cdot(\mathbf{u}_I-\mathbf{u}_J)e^{i\mathbf{q}\cdot(\mathbf{R}_I-\mathbf{R}_J)}. \end{aligned} \tag{4}$$

Let us multiply this equation by $e^{-i\mathbf{k}\cdot\mathbf{R}_I}$ and sum over $I$. In this way, we switch from motion of individual ions, described by $\mathbf{u}_I$, to collective ion oscillations, specified by the wavevector $\mathbf{k}$ and a new variable $\mathbf{A}_\mathbf{k} \equiv \sqrt{m/N}\sum_I \mathbf{u}_I e^{-i\mathbf{k}\cdot\mathbf{R}_I}$ ($N$ is the total number of ions, and we focus on the case where there is only one ion in the lattice primitive cell). We assume the periodic dependence of $\mathbf{A}_\mathbf{k} \propto e^{-i\omega_\mathbf{k}t}$ on time so that $\ddot{\mathbf{A}}_\mathbf{k} = -\omega_\mathbf{k}^2\mathbf{A}_\mathbf{k}$. Then, the equation of motion takes the form

$$\begin{aligned} \omega_\mathbf{k}^2\mathbf{A}_\mathbf{k} = &\frac{\omega_{\rm p}^2}{n(2\pi)^3}\int\frac{\mathrm{d}\mathbf{q}}{q^2\epsilon(\mathbf{q})}i\mathbf{q}(i\mathbf{q}\cdot\mathbf{A}_\mathbf{k}) \\ &\times\sum_{I\neq 0} e^{i\mathbf{q}\cdot\mathbf{R}_I}(1-e^{-i\mathbf{k}\cdot\mathbf{R}_I}), \end{aligned} \tag{5}$$

which can be rewritten as a system of linear equations [e.g., Eq. (17) of Ref. 13]

$$\omega_\mathbf{k}^2 A_{\mathbf{k}\mu} = D_{\mu\nu}(\mathbf{k})A_{\mathbf{k}\nu}, \tag{6}$$

$$\begin{aligned} D_{\mu\nu}(\mathbf{k}) = &\frac{\omega_{\rm p}^2}{n(2\pi)^3}\frac{\partial^2}{\partial X_\mu\partial X_\nu} \\ &\times\sum_{I\neq 0}(1-e^{-i\mathbf{k}\cdot\mathbf{R}_I})\int\frac{\mathrm{d}\mathbf{q}}{q^2\epsilon(\mathbf{q})}e^{i\mathbf{q}\cdot(\mathbf{R}_I-\mathbf{X})}|_{\mathbf{X}=0}. \end{aligned} \tag{7}$$

In this case, $\omega_{\rm p} = \sqrt{4\pi n Z^2e^2/m}$ is the ion plasma frequency and $D_{\mu\nu}(\mathbf{k})$ is the dynamic matrix.

If a magnetic field $\mathbf{B} \equiv \mathbf{h}B$ is turned on ($\mathbf{h}$ is the unit vector in the direction of the field), then on the right-hand side of Eq. (4), the Lorentz force $Z|e|\dot{\mathbf{u}}_I \times \mathbf{B}$ appears. Upon transition to the $\mathbf{k}$-space, we thus arrive at

$$D_{\mu\nu}(\mathbf{k})A_{\mathbf{k}\nu} - \Omega_\mathbf{k}^2 A_{\mathbf{k}\mu} - i\Omega_\mathbf{k}\omega_{\rm B}\varepsilon_{\mu\nu\lambda}h_\nu A_{\mathbf{k}\lambda} = 0, \tag{8}$$

where $\omega_{\rm B} = Z|e|B/(mc)$ is the ion cyclotron frequency and $\varepsilon_{\mu\nu\lambda}$ is the Levi-Civita symbol, and we have adopted a

convention that a capital Ω denoted frequencies in the presence of a magnetic field, while a lowercase $\omega$ stands for the non-magnetized frequencies. This result coincides with Eq. (9) of Ref. 14 except that the dynamic matrix $D_{\mu\nu}$ is now modified by the polarization. Our goal is to analyze solutions of Eq. (8).

## III. PHONON SPECTRUM

### A. Ideal Coulomb crystal

To begin with, let us recall the main features of the Coulomb crystal phonon spectrum in the absence of the magnetic field and electron polarization. For a crystal with one ion in the lattice primitive cell, such as the bcc crystal, there are three phonon modes at each $\mathbf{k}$ in the first Brillouin zone. At small $k$ [i.e., for $ka \ll 1$ where $a = (4\pi n/3)^{-1/3}$ is the ion sphere radius, $k = |\mathbf{k}|$, and $\mathbf{k} \equiv k\hat{\mathbf{k}}$], the dynamic matrix can be expanded[3] as

$$\frac{D_{\mu\nu}(\mathbf{k})}{\omega_{\rm p}^2} = \frac{k_\mu k_\nu}{k^2} - \frac{(ka_1)^2}{16\pi}\left(\alpha\frac{k_\mu k_\nu}{k^2} + \beta\delta_{\mu\nu} + \gamma_{\mu\nu\rho\sigma}\frac{k_\rho k_\sigma}{k^2}\right). \quad (9)$$

Hereafter, the Cartesian coordinates denoted by Greek indices refer to the reference frame $xyz$ associated with the bcc lattice unit cell. This reference frame is oriented in such a way that an irreducible part of the bcc lattice first Brillouin zone can be defined by inequalities $k_x \geq k_y \geq k_z \geq 0$ and $k_x + k_y \leq 2\pi/a_1$. Furthermore, $a_1$ is the lattice constant, $na_1^3 = 2$ for the bcc lattice, and $\alpha$, $\beta$, and $\gamma_{\mu\nu\rho\sigma}$ are lattice parameters introduced and calculated in Ref. 3 (see also Ref. 14 for updated values).

The dispersion equation then can be cast in the form[15]

$$-\frac{\omega^6}{\omega_{\rm p}^6} + \frac{\omega^4}{\omega_{\rm p}^4} + E_0\frac{\omega^2}{\omega_{\rm p}^2} + F_0 = 0, \quad (10)$$

where expressions for $E_0$ and $F_0$ are somewhat lengthy and are given, e.g., in Eq. (13) of Ref. 14. It is important that $E_0 \propto k^2$ and $F_0 \propto k^4$, and thus, two of the modes are acoustic: $\omega_{1,2} = c_{1,2}k$ at small $k$, while the third one is optic: $\omega_3 = \omega_{\rm p} > 0$ at $k = 0$ (as usual, we enumerate non-magnetized modes by a lower index running from 1 to 3; $c_{1,2}$ are the corresponding sound velocities).

More explicitly, at small $k$,

$$\frac{16\pi\omega_{1,2}^2}{\omega_{\rm p}^2(ka_1)^2} = \zeta - \frac{\eta}{k^4}(k_x^2k_y^2 + k_y^2k_z^2 + k_z^2k_x^2) \pm \frac{\eta S}{k^4}, \quad (11)$$

where $S \equiv \sqrt{k_x^4k_y^4 + k_y^4k_z^4 + k_z^4k_x^4 - k^2k_x^2k_y^2k_z^2}$, $\zeta \equiv -\beta - \gamma_{xxyy}$, and $\eta \equiv \gamma_{xxxx} - 3\gamma_{xxyy}$. Since at all $\mathbf{k}$ frequencies satisfy the sum rule $\sum_{i=1}^3 \omega_i^2 = \omega_{\rm p}^2$, $\omega_3$ can be immediately deduced. All frequencies are of the same order at or near the outer Brillouin zone boundaries. In Fig. 1(a), the modes of such a crystal are plotted by solid (black) curves as functions of $ka$ with $\hat{\mathbf{k}} = (1,1,0)/\sqrt{2}$. The behavior of the modes in any other direction is qualitatively the same with the exception of $\hat{\mathbf{k}} = (1,0,0)$ and $\hat{\mathbf{k}} = (1,1,1)/\sqrt{3}$, where the two acoustic modes coincide.

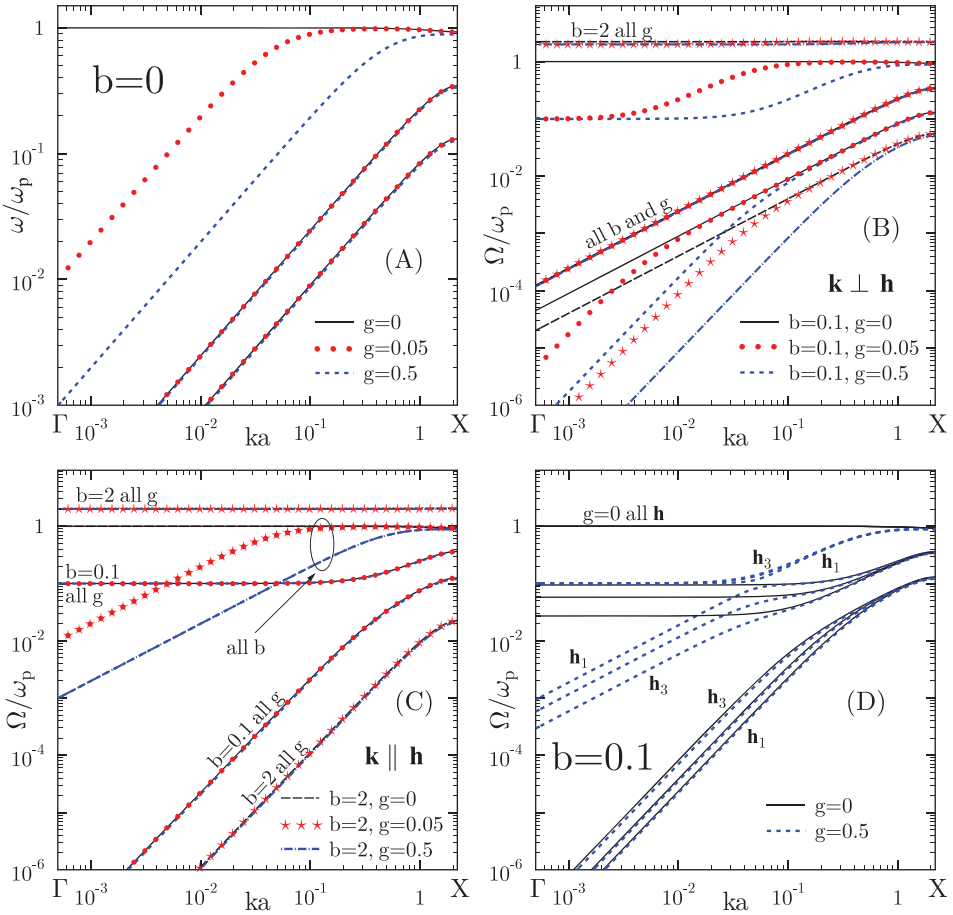


FIG. 1. Dispersion curves of the bcc lattice along the Γ$X$ edge of the irreducible part of the first Brillouin zone, $\hat{\mathbf{k}} = (1,1,0)/\sqrt{2}$, for $g \equiv \kappa_{\rm TF}a = 0$, 0.05, and 0.5. The magnetic field is absent in panel A; $b \equiv \omega_{\rm B}/\omega_{\rm p} = 0.1$ and 2 and $\mathbf{h} = (0,0,1)$ (orthogonal propagation) in panel B; $b = 0.1$ and 2 and $\mathbf{h} = (1,1,0)/\sqrt{2}$ (parallel propagation) in panel C. Panels B and C have the same curve types and share the legend. Panel D shows the evolution of the modes with the angle between $\hat{\mathbf{k}}$ and $\mathbf{h}$ for $b = 0.1$ and $g = 0$ and 0.5. In this case, $\mathbf{h}_1 = (2/3, 2/3, 1/3)$ and $\mathbf{h}_3 = (1,1,5)/\sqrt{27}$. Curves with $\mathbf{h}_2 = (1,1,2)/\sqrt{6}$ are not marked but always lie between respective curves for $\mathbf{h}_1$ and $\mathbf{h}_3$.

Polarization vectors of the bcc Coulomb crystal with a rigid background and without a magnetic field are also well-known.[4] In particular, at small $k$, one needs to find algebraic cofactors for any row of the matrix $D_{\mu\nu}-\omega_{1,2}^2\delta_{\mu\nu}$. For a more symmetric form, one can find cofactors for all three rows and add them together. This produces non-normalized (denoted by a tilde) polarization vectors of the two acoustic modes

$$\begin{aligned}\tilde{e}_{1,2x} &= k_y^2k_z^2(k_y^2+k_z^2)+k_x(k_x^2-k_yk_z)(k_y^3+k_z^3)\\ &\quad -k_x^2(k_y^4+k_z^4)\pm\left[k_y^2+k_z^2-k_x(k_y+k_z)\right]S,\\ \tilde{e}_{1,2y} &= k_x^2k_z^2(k_x^2+k_z^2)+k_y(k_y^2-k_xk_z)(k_x^3+k_z^3)\\ &\quad -k_y^2(k_x^4+k_z^4)\pm\left[k_x^2+k_z^2-k_y(k_x+k_z)\right]S,\\ \tilde{e}_{1,2z} &= k_x^2k_y^2(k_x^2+k_y^2)+k_z(k_z^2-k_xk_y)(k_x^3+k_y^3)\\ &\quad -k_z^2(k_x^4+k_y^4)\pm\left[k_x^2+k_y^2-k_z(k_x+k_y)\right]S. \end{aligned}\tag{12}$$

It is easy to check that $\tilde{\mathbf{e}}_1\perp\tilde{\mathbf{e}}_2$ and $\tilde{\mathbf{e}}_{1,2}\perp\mathbf{k}$, and therefore, the polarization vector of the optic mode ($\omega_3\approx\omega_\mathrm{p}$) is $\mathbf{e}_3=\hat{\mathbf{k}}$. Normalized polarization vectors $\mathbf{e}_{1,2}=\tilde{\mathbf{e}}_{1,2}/|\tilde{\mathbf{e}}_{1,2}|$.

### B. Coulomb crystal with a polarizable background

If the electron polarization is taken into account, an expression analogous to Eq. (9) can be obtained at small $k$ provided the polarization parameter $g\equiv\kappa_\mathrm{TF}a\ll1$. An analysis of Eqs. (18) and (19) of Ref. 13 indicates that the polarization alters significantly the $G=0$ term of the dynamic matrix lattice sum and also gives rise to corrections to other terms of the lattice sum at most of the order $O(k^2\kappa_\mathrm{TF}^2), O(k^4)$ or $O(\kappa_\mathrm{TF}^4)$, which may be neglected. This results in

$$\frac{D_{\mu\nu}(\mathbf{k})}{\omega_\mathrm{p}^2}=\xi\frac{k_\mu k_\nu}{k^2}-\frac{(ka_\mathrm{I})^2}{16\pi}\left(\alpha\frac{k_\mu k_\nu}{k^2}+\beta\delta_{\mu\nu}+\gamma_{\mu\nu\rho\sigma}\frac{k_\rho k_\sigma}{k^2}\right),\tag{13}$$

in place of Eq. (9), while Eq. (10) becomes

$$-\frac{\omega^6}{\omega_\mathrm{p}^6}+\xi\left(\frac{\omega^4}{\omega_\mathrm{p}^4}+E_0\frac{\omega^2}{\omega_\mathrm{p}^2}+F_0\right)=0,\tag{14}$$

where $\xi\equiv k^2/(k^2+\kappa_\mathrm{TF}^2)$. Clearly, if $1-\xi\ll1$, the modes are not affected. In general, the sum rule becomes $k$-dependent and reads (to the main order) $\sum_{i=1}^3\omega_i^2\approx\xi\omega_\mathrm{p}^2$, which means that as $k\to0$, all modes, including $\omega_3$, tend to zero. Finally, simple estimates show that $c_{1,2}\ll\omega_\mathrm{p}/\kappa_\mathrm{TF}$. This allows one to conclude[5] that the two acoustic modes $\omega_{1,2}$ are virtually unaffected by electron polarization, but the optic mode is converted into an acoustic one at $k<\kappa_\mathrm{TF}$: $\omega_3\approx\sqrt{\xi}\omega_\mathrm{p}$. These modes are also plotted in Fig. 1(a) for weak ($g=0.05$) and moderate ($g=0.5$) electron polarizability by (red) dots and dashed (blue) curves, respectively.

The polarization vectors $\mathbf{e}_{1,2}$ do not change, to the main order in $g$, because all algebraic cofactors differ from the rigid background case by the same multiplier $\xi$. Thus, at small $k$ modes, $\omega_{1,2}$ continue to be transverse with respect to $\mathbf{k}$, while the third mode remains longitudinal.

### C. Magnetized Coulomb crystal with the rigid background

If the magnetic field is turned on while the polarization is off, the dispersion equation at $ka\ll1$ becomes

$$-\frac{\Omega^6}{\omega_\mathrm{p}^6}+(1+b^2)\frac{\Omega^4}{\omega_\mathrm{p}^4}+E_B\frac{\Omega^2}{\omega_\mathrm{p}^2}+F_0=0.\tag{15}$$

In this case, $b\equiv\omega_\mathrm{B}/\omega_\mathrm{p}$ is the magnetization parameter and $E_B$ is given in Eq. (12) of Ref. 14. The sum rule is modified as $\sum_{i=1}^3\Omega^{(i)2}=\omega_\mathrm{p}^2+\omega_\mathrm{B}^2$ (we enumerate magnetized modes by an upper index in parenthesis running from 1 to 3), and a more complex picture emerges.

If the magnetic field is directed along one of the vectors $\mathbf{e}_m$ above, one of the magnetized frequencies, say $\Omega^{(m)}=\omega_m$, while the other two satisfy

$$\Omega^{(n,l)2}\omega_\mathrm{B}^2=\left(\omega_n^2-\Omega^{(n,l)2}\right)\left(\omega_l^2-\Omega^{(n,l)2}\right),\tag{16}$$

where $m\neq n\neq l\neq m$ (in general, there is no relationship between numerical indices of frequencies $\omega$ and $\Omega$, so that given $\omega_n$ and $\omega_l$, $n\neq l$, it does not matter which of the magnetized frequencies is designated $\Omega^{(n)}$ and which $\Omega^{(l)}$).

At small $k$, if $\mathbf{h}=\mathbf{e}_1$ (orthogonal propagation), $\Omega^{(1)}=c_1k$, $\Omega^{(2)}=c_2k/\sqrt{1+b^2}$, and $\Omega^{(3)}=\sqrt{\omega_\mathrm{p}^2+\omega_\mathrm{B}^2}$. Likewise, if $\mathbf{h}=\mathbf{e}_2$, $\Omega^{(1)}=c_1k/\sqrt{1+b^2}$, $\Omega^{(2)}=c_2k$, and $\Omega^{(3)}=\sqrt{\omega_\mathrm{p}^2+\omega_\mathrm{B}^2}$. Further analysis[14] shows that for orthogonal propagation with the magnetic field oriented arbitrarily in the plane perpendicular to $\mathbf{k}$, there are still two acoustic modes and an optic one with the hybrid frequency $\Omega^{(3)}=\sqrt{\omega_\mathrm{p}^2+\omega_\mathrm{B}^2}$ at $k=0$. These modes are shown by solid and long-dashed (black) curves in Fig. 1(b) for $b=0.1$ and 2, respectively. For an oblique propagation, the two acoustic modes are modified in the vicinity of the Brillouin zone center. One of them becomes quadratic ($\Omega\propto k^2$), and the other one becomes optic. This is illustrated by solid (black) curves in Fig. 1(d) for $b=0.1$. The third mode remains optic with a somewhat reduced frequency to maintain the sum rule. As the angle between the wavevector and the field line decreases, the region expands, where the acoustic modes are modified, and may spread out, for $b\gg1$, over the entire Brillouin zone. If, at small k, $\mathbf{h}=\mathbf{e}_3=\hat{\mathbf{k}}$ (parallel propagation), then $\Omega^{(1)}=\omega_\mathrm{B}$, $\Omega^{(2)}=c_1c_2k^2/\omega_\mathrm{B}$, and $\Omega^{(3)}=\omega_3=\omega_\mathrm{p}$ [cf. solid and long-dashed (black) curves in Fig. 1(c)]. Finally, it is worth mentioning that if $\omega_\mathrm{B}\gg\omega_\mathrm{p}$, the three magnetized frequencies are widely spaced from each other across the entire Brillouin zone.

### D. Magnetized Coulomb crystal with a polarizable background

We can now turn on the magnetic field and the electron polarization simultaneously. As mentioned in Sec. II, the functional form of the Thomas-Fermi dielectric function is not affected by the magnetic field. At any $\mathbf{k}$, the phonon spectrum of the system can be obtained by solving the dispersion equation

$$\det\left\{D_{\mu\nu}(\mathbf{k}) - \Omega^2\delta_{\mu\nu} - i\Omega\omega_{\rm B}\varepsilon_{\mu\lambda\nu}h_\lambda\right\} = 0\,, \qquad (17)$$

where $D_{\mu\nu}(\mathbf{k})$ is given by Eq. (7).

The spectrum of the bcc lattice still consists of three modes. At small $k$, the dispersion equation can be derived by an appropriate expansion of Eq. (17). Alternatively, it can be obtained from Eq. (14) by analyzing the relationship between Eqs. (10) and (15). In particular, it is clear that the coefficients of the $\Omega^6$ and $\Omega^0$ terms in Eq. (15) are the same as in the field-free case, whereas the coefficient of the $\Omega^4$ term is equal to the trace of the dynamic matrix, divided by $\omega_{\rm p}^2$, plus $b^2$. This can be easily extended to the case with electron polarization. The hardest part is the coefficient $E_B$ in Eq. (15), which is a sum of three terms. They are *(i)* the $\omega^2$ coefficient in Eq. (10), *(ii)* the contraction of the first, $O(k^0)$, term on the right-hand side of Eq. (9) with two factors $i\Omega\omega_{\rm B}\varepsilon_{\mu\lambda\nu}h_\lambda$, representing the magnetic field effect, and *(iii)* the contraction of the $\propto (ka_{\rm I})^2$ term on the right-hand side of Eq. (9) with the same factors. Consequently, once polarization is included, the first and second contributions to $E_B$ must be multiplied by $\xi$, while the third one does not change. This reasoning results in the following equation:

$$-\frac{\Omega^6}{\omega_{\rm p}^6} + (\xi + b^2)\frac{\Omega^4}{\omega_{\rm p}^4} + \left\{E_B + (\xi - 1)\left[E_0 - b^2(\hat{\mathbf{k}}\cdot\mathbf{h})^2\right]\right\} \times \frac{\Omega^2}{\omega_{\rm p}^2} + \xi F_0 = 0\,. \qquad (18)$$

The phonon modes can be easily analyzed at $1 - \xi \ll 1$ and $\xi \ll 1$. In the former case, Eq. (18) reduces to Eq. (15), which simply means that the magnetized modes with polarization must merge into the modes of the magnetized crystal with the rigid background at sufficiently large $k$. This is seen very well in Figs. 1(b) and 1(c) where (red) dots and stars representing $g = 0.05$ merge with rigid background modes at smaller $k$ than (blue) dashes and dot-dashes representing $g = 0.5$.

Consider now $\xi \ll 1$ or $k \ll \kappa_{\rm TF}$. We can gain some insights into the modes by again directing the magnetic field along field-free polarization vectors $\mathbf{e}_i$. If $\mathbf{h} = \mathbf{e}_3$ [parallel propagation, Fig. 1(c)], the cyclotron mode $\Omega^{(1)}$ and the soft quadratic mode $\Omega^{(2)}$ do not change, but the other optic mode gets converted into an acoustic one $\Omega^{(3)} = \omega_3 = \sqrt{\xi}\omega_{\rm p}$ as expected. Interestingly, for $b < 1$, this results in a mode crossing seen in Fig. 1(c). The crossing becomes an anti-crossing as soon as the angle between $\hat{\mathbf{k}}$ and $\mathbf{h}$ departs from zero [Fig. 1(d)]. For orthogonal propagation [e.g., Fig. 1(b)], some new features emerge. Specifically, if $\mathbf{h} = \mathbf{e}_1$, $\Omega^{(1)} = c_1 k$, $\Omega^{(2)} = c_2 k/\sqrt{1 + b^2/\xi}$, which becomes quadratic at sufficiently small $\xi$, and $\Omega^{(3)} = \sqrt{\xi\omega_{\rm p}^2 + \omega_{\rm B}^2}$, which tends to cyclotron frequency $\omega_{\rm B}$ as $k \to 0$. Likewise, if $\mathbf{h} = \mathbf{e}_2$, $\Omega^{(1)} = c_1 k/\sqrt{1 + b^2/\xi}$, $\Omega^{(2)} = c_2 k$, and $\Omega^{(3)} = \sqrt{\xi\omega_{\rm p}^2 + \omega_{\rm B}^2}$.

For a more general angle of propagation [cf. Fig. 1(d)], we can rewrite Eq. (18) as

$$-\frac{\Omega^6}{\omega_{\rm p}^6} + b^2\frac{\Omega^4}{\omega_{\rm p}^4} - \frac{b^2k^2}{\kappa_{\rm TF}^2}\left[C(\hat{\mathbf{k}},\mathbf{h})\kappa_{\rm TF}^2 + (\hat{\mathbf{k}}\cdot\mathbf{h})^2\right] \times \frac{\Omega^2}{\omega_{\rm p}^2} + \frac{k^2}{\kappa_{\rm TF}^2}F_0 = 0\,, \qquad (19)$$

where $-C(\hat{\mathbf{k}},\mathbf{h})b^2k^2 \equiv E_B - E_0 + b^2(\hat{\mathbf{k}}\cdot\mathbf{h})^2$ so that $C(\hat{\mathbf{k}},\mathbf{h})$ is independent of $k$, $b$, and $\kappa_{\rm TF}$. An analysis shows that the quantity in square brackets is always greater than zero. Taking into account the degree of $k$ in various terms, the frequencies are now approximately given by the ratios of the equation coefficients

$$\frac{\Omega^2}{\omega_{\rm p}^2} \approx \frac{F_0}{b^2\left[C(\hat{\mathbf{k}},\mathbf{h})\kappa_{\rm TF}^2 + (\hat{\mathbf{k}}\cdot\mathbf{h})^2\right]}\,, \qquad (20)$$

which interpolates between $\Omega^{(2)}$ for parallel propagation and $\Omega^{(2,1)}$ for orthogonal propagation with $\mathbf{h} = \mathbf{e}_{1,2}$;

$$\frac{\Omega^2}{\omega_{\rm p}^2} \approx \frac{k^2}{\kappa_{\rm TF}^2}\left[C(\hat{\mathbf{k}},\mathbf{h})\kappa_{\rm TF}^2 + (\hat{\mathbf{k}}\cdot\mathbf{h})^2\right]\,, \qquad (21)$$

which interpolates between $\Omega^{(3)}$ for parallel propagation and $\Omega^{(1,2)}$ for orthogonal propagation with $\mathbf{h} = \mathbf{e}_{1,2}$; and

$$\frac{\Omega^2}{\omega_{\rm p}^2} \approx b^2\,, \qquad (22)$$

which reduces to $\Omega^{(1)}$ for parallel propagation and to $\Omega^{(3)}$ for orthogonal propagation. These transitions are illustrated by the evolution of dashed (blue) curves in Figs. 1(b)–1(d).

Summarizing, we see that for orthogonal propagation, there is always a quadratic mode $\Omega \propto k^2/(b\kappa_{\rm TF})$ and an acoustic mode $\Omega \propto k$ independent of $b$ and $\kappa_{\rm TF}$. For parallel propagation, there is a quadratic mode $\Omega \propto k^2/b$ and an acoustic mode $\Omega \propto k/\kappa_{\rm TF}$. For any angle of propagation, there is a cyclotron mode $\Omega \approx \omega_{\rm B}$.

## IV. QUANTIZATION OF THE ION MOTION

In this section, we quantize the ion motion in the magnetized Coulomb crystal with a polarizable electron background and express ion displacement operators in terms of phonon creation and annihilation operators. We follow the approach of Ref. 6, but, for the sake of clarity, we write out explicitly certain intermediate steps omitted in their derivation.

It is advantageous to switch from the Cartesian reference system $xyz$, associated with the bcc lattice unit cell, to the Cartesian reference system with eigenvectors[16] of the dynamic matrix $\mathbf{e}_{\mathbf{k}1,2,3}$ as a basis. The basis is then different for each $\mathbf{k}$, and we use lower Latin indices to denote coordinates in this basis. Hamiltonian of the ion vibrations reads

$$H = \frac{1}{2}\sum_{\mathbf{k}l}\left(\pi_{-\mathbf{k}l}\pi_{\mathbf{k}l} + \omega_{\mathbf{k}l}^2 A_{\mathbf{k}l}A_{-\mathbf{k}l}\right)\,, \qquad (23)$$

where $\boldsymbol{\pi}_{\mathbf{k}} = \dot{\mathbf{A}}_{-\mathbf{k}}$. Canonical conjugate momentum to $\mathbf{A}_{\mathbf{k}}$ is $\mathbf{P}_{\mathbf{k}} = \boldsymbol{\pi}_{\mathbf{k}} + \omega_{\rm B}[\mathbf{h}\times\mathbf{A}_{-\mathbf{k}}]/2$.

Applying the canonical quantization procedure to $A_{\mathbf{k}l}$ and $P_{\mathbf{k}l}$, we obtain from Eq. (23) the respective quantum mechanical Hamiltonian $\hat{H}$, which needs to be diagonalized. Accordingly, we require $[\hat{H}, \hat{a}^\dagger_{\mathbf{k}}] = \Omega_{\mathbf{k}}\hat{a}^\dagger_{\mathbf{k}}$, where $\hat{a}^\dagger_{\mathbf{k}}$ is the creation operator of a magnetized phonon with wavevector $\mathbf{k}$. It can be looked for in the form

$$\hat{a}^\dagger_{\mathbf{k}} = \sum_l \left(\alpha_{\mathbf{k}l}\hat{\pi}_{\mathbf{k}l} + \beta_{\mathbf{k}l}\hat{A}_{-\mathbf{k}l}\right), \tag{24}$$

where $\alpha_{\mathbf{k}l}$ and $\beta_{\mathbf{k}l}$ are unknown complex coefficients. This results in the system of equations

$$(\omega^2_{\mathbf{k}l} - \Omega^2_{\mathbf{k}})\alpha_{\mathbf{k}l} - i\Omega_{\mathbf{k}}\omega_{\mathrm{B}}\sum_{mn}\varepsilon_{lmn}h_m\alpha_{\mathbf{k}n} = 0, \tag{25}$$

$$\beta_{\mathbf{k}l} = \frac{i\omega^2_{\mathbf{k}l}}{\Omega_{\mathbf{k}}}\alpha_{\mathbf{k}l}\,. \tag{26}$$

Equation (25) coincides with Eq. (8) if the latter is written in the basis of eigenvectors of $D_{\mu\nu}$. Since $\omega_{\mathbf{k}l} = \omega_{-\mathbf{k}l}$, the coefficients $\alpha_{\mathbf{k}l}$ and $\alpha_{-\mathbf{k}l}$ can be set equal. There are three solutions of Eq. (25), $\Omega^{(i)}_{\mathbf{k}}$ and $\boldsymbol{\alpha}^{(i)}_{\mathbf{k}}$, $i = 1$, 2, and 3, and, consequently, three different creation operators corresponding to three different modes at given $\mathbf{k}$

$$\hat{a}^{(i)\dagger}_{\mathbf{k}} = \sum_l \alpha^{(i)}_{\mathbf{k}l}\left(\hat{\pi}_{\mathbf{k}l} + \frac{i\omega^2_{\mathbf{k}l}}{\Omega^{(i)}_{\mathbf{k}}}\hat{A}_{-\mathbf{k}l}\right). \tag{27}$$

Multiplying Eq. (25) (at a fixed $i$) either by $\alpha^{(j)*}_{\mathbf{k}l}$ or by $\alpha^{(j)}_{\mathbf{k}l}$ and summing over $l$, we obtain "orthogonality" conditions for the $\alpha$-coefficients

$$\sum_l \alpha^{(j)*}_{\mathbf{k}l}\alpha^{(i)}_{\mathbf{k}l}(\omega^2_{\mathbf{k}l} + \Omega^{(i)}_{\mathbf{k}}\Omega^{(j)}_{\mathbf{k}})\left(1 - \frac{\Omega^{(i)}_{\mathbf{k}}}{\Omega^{(j)}_{\mathbf{k}}}\right) = 0,$$

$$\sum_l \alpha^{(j)}_{\mathbf{k}l}\alpha^{(i)}_{\mathbf{k}l}(\omega^2_{\mathbf{k}l} - \Omega^{(i)}_{\mathbf{k}}\Omega^{(j)}_{\mathbf{k}})\left(1 + \frac{\Omega^{(i)}_{\mathbf{k}}}{\Omega^{(j)}_{\mathbf{k}}}\right) = 0. \tag{28}$$

Let us evaluate the commutator

$$\left[\hat{a}^{(i)}_{\mathbf{k}}, \hat{a}^{(j)\dagger}_{\mathbf{k}}\right] = \sum_l \alpha^{(i)*}_{\mathbf{k}l}\alpha^{(j)}_{\mathbf{k}l}\left(\omega^2_{\mathbf{k}l} + \Omega^{(i)}_{\mathbf{k}}\Omega^{(j)}_{\mathbf{k}}\right)\frac{1}{\Omega^{(i)}_{\mathbf{k}}}, \tag{29}$$

which must be equal to $\delta_{ij}$. Using the first one of Eq. (28), we see that the right-hand side of Eq. (29) is zero for $\Omega^{(i)}_{\mathbf{k}} \neq \Omega^{(j)}_{\mathbf{k}}$. In the opposite case, we arrive at the normalization condition

$$\sum_l \alpha^{(i)*}_{\mathbf{k}l}\alpha^{(i)}_{\mathbf{k}l}\left(\frac{\omega^2_{\mathbf{k}l}}{\Omega^{(i)}_{\mathbf{k}}} + \Omega^{(i)}_{\mathbf{k}}\right) = 1. \tag{30}$$

The inverse transformation can be looked for in the form

$$\hat{A}_{-\mathbf{k}l} = \sum_i \left(\gamma^{(i)}_{\mathbf{k}l}\hat{a}^{(i)\dagger}_{\mathbf{k}} + \delta^{(i)}_{\mathbf{k}l}\hat{a}^{(i)}_{-\mathbf{k}}\right),$$

$$\hat{\pi}_{\mathbf{k}l} = \sum_i \left(\phi^{(i)}_{\mathbf{k}l}\hat{a}^{(i)\dagger}_{\mathbf{k}} + \chi^{(i)}_{\mathbf{k}l}\hat{a}^{(i)}_{-\mathbf{k}}\right). \tag{31}$$

Since $[\hat{H}, \hat{A}_{-\mathbf{k}l}] = -i\pi_{\mathbf{k}l}$, $\phi^{(i)}_{\mathbf{k}l} = i\Omega^{(i)}_{\mathbf{k}}\gamma^{(i)}_{\mathbf{k}l}$ and $\chi^{(i)}_{\mathbf{k}l} = -i\Omega^{(i)}_{\mathbf{k}}\delta^{(i)}_{\mathbf{k}l}$. Also, $[\hat{H}, \hat{\pi}_{\mathbf{k}l}] = i\omega^2_{\mathbf{k}l}\hat{A}_{-\mathbf{k}l} + i\omega_{\mathrm{B}}\sum_{mn}\varepsilon_{lmn}h_m\hat{\pi}_{\mathbf{k}n}$, which produces

$$(\omega^2_{\mathbf{k}l} - \Omega^{(i)2}_{\mathbf{k}})\gamma^{(i)}_{\mathbf{k}l} + i\Omega^{(i)}_{\mathbf{k}}\omega_{\mathrm{B}}\sum_{mn}\varepsilon_{lmn}h_m\gamma^{(i)}_{\mathbf{k}n} = 0,$$

$$(\omega^2_{\mathbf{k}l} - \Omega^{(i)2}_{\mathbf{k}})\delta^{(i)}_{\mathbf{k}l} - i\Omega^{(i)}_{\mathbf{k}}\omega_{\mathrm{B}}\sum_{mn}\varepsilon_{lmn}h_m\delta^{(i)}_{\mathbf{k}n} = 0. \tag{32}$$

Therefore, $\delta^{(i)}_{\mathbf{k}l} \propto \alpha^{(i)}_{\mathbf{k}l}$ and $\gamma^{(i)}_{\mathbf{k}l} \propto \alpha^{(i)*}_{\mathbf{k}l}$, and combining Eqs. (27) and (31) and the second one of Eq. (28), we conclude that $\gamma^{(i)}_{\mathbf{k}l} = -i\alpha^{(i)*}_{\mathbf{k}l}$. Analogously, substituting the inverse transformations (31) into

$$\hat{a}^{(i)}_{-\mathbf{k}} = \sum_l \alpha^{(i)*}_{\mathbf{k}l}\left(\hat{\pi}_{\mathbf{k}l} - \frac{i\omega^2_{\mathbf{k}l}}{\Omega^{(i)}_{\mathbf{k}}}\hat{A}_{-\mathbf{k}l}\right), \tag{33}$$

we observe that $\delta^{(i)}_{\mathbf{k}l} = i\alpha^{(i)}_{\mathbf{k}l}$. The inverse transformation thus reads

$$\hat{A}_{-\mathbf{k}l} = -i\sum_i \left(\alpha^{(i)*}_{\mathbf{k}l}\hat{a}^{(i)\dagger}_{\mathbf{k}} - \alpha^{(i)}_{\mathbf{k}l}\hat{a}^{(i)}_{-\mathbf{k}}\right),$$

$$\hat{\pi}_{\mathbf{k}l} = \sum_i \Omega^{(i)}_{\mathbf{k}}\left(\alpha^{(i)*}_{\mathbf{k}l}\hat{a}^{(i)\dagger}_{\mathbf{k}} + \alpha^{(i)}_{\mathbf{k}l}\hat{a}^{(i)}_{-\mathbf{k}}\right). \tag{34}$$

Substituting Eqs. (27) and (33) into Eq. (34), we obtain "completeness" conditions for the $\alpha$-coefficients

$$\delta_{lm} = \sum_i \frac{\omega_{\mathbf{k}l}\omega_{\mathbf{k}m}}{\Omega^{(i)}_{\mathbf{k}}}(\alpha^{(i)*}_{\mathbf{k}l}\alpha^{(i)}_{\mathbf{k}m} + \alpha^{(i)}_{\mathbf{k}l}\alpha^{(i)*}_{\mathbf{k}m}),$$

$$\delta_{lm} = \sum_i \Omega^{(i)}_{\mathbf{k}}(\alpha^{(i)*}_{\mathbf{k}l}\alpha^{(i)}_{\mathbf{k}m} + \alpha^{(i)}_{\mathbf{k}l}\alpha^{(i)*}_{\mathbf{k}m}),$$

$$0 = \sum_i (\alpha^{(i)*}_{\mathbf{k}l}\alpha^{(i)}_{\mathbf{k}m} - \alpha^{(i)}_{\mathbf{k}l}\alpha^{(i)*}_{\mathbf{k}m}). \tag{35}$$

## V. POLARIZATION OF THE MAGNETIZED PHONON MODES

In this section, we evaluate the $\alpha$-coefficients and characterize the direction of the ion motion in various magnetized modes. The non-normalized $\tilde{\boldsymbol{\alpha}}^{(i)}$ coefficients[17] are obtained as algebraic cofactors to any row of the matrix $Q^{(i)}_{mn} \equiv (\omega^2_m - \Omega^{(i)2})\delta_{mn} + \sum_l i\Omega^{(i)}\omega_{\mathrm{B}}\varepsilon_{mnl}h_l$. Calculating algebraic cofactors for all three rows and adding them together result in

$$\tilde{\boldsymbol{\alpha}}^{(i)} = \sum_m \tilde{\alpha}^{(i)}_m\mathbf{e}_m = \sum_m \mathbf{e}_m\left\{\frac{1}{2}\sum_{nl}|\varepsilon_{mnl}|\left(\omega^2_n - \Omega^{(i)2}\right)\right.$$
$$\times\left(\omega^2_l - \Omega^{(i)2}\right) - \Omega^{(i)2}\omega^2_{\mathrm{B}}h_m\sum_l h_l$$
$$\left. + i\Omega^{(i)}\omega_{\mathrm{B}}\sum_{nl}\varepsilon_{mnl}h_n\left(\omega^2_n - \Omega^{(i)2}\right)\right\} \equiv \tilde{\boldsymbol{\alpha}}^{(i)}_R + i\tilde{\boldsymbol{\alpha}}^{(i)}_I. \tag{36}$$

This represents elliptically polarized motion in the plane spanned by vectors $\tilde{\boldsymbol{\alpha}}^{(i)}_R$ and $\tilde{\boldsymbol{\alpha}}^{(i)}_I$.

Equation (36) can be simplified if the magnetic field is directed along one of the polarization vectors $\mathbf{e}_m$ ($m = 1$, 2, and 3). In this case, as discussed near Eq. (16), $\Omega^{(m)} = \omega_m$, and thus

$$\tilde{\alpha}^{(m)}_m = (\omega^2_n - \omega^2_m)(\omega^2_l - \omega^2_m) - \omega^2_m\omega^2_{\mathrm{B}}, \quad \tilde{\alpha}^{(m)}_{n,l} = 0, \tag{37}$$

where $m \neq n \neq l \neq m$ and $h_{n,l} = 0$. This describes a linearly polarized oscillation along the magnetic field. The

normalized coefficient satisfying Eq. (30) becomes $\boldsymbol{\alpha}^{(m)} = \mathbf{e}_m/\sqrt{2\omega_m}$.

Now, let us focus on $\boldsymbol{\alpha}^{(n,l)}$. Cancellation of the first and second terms in curly brackets in Eq. (36) ensures that $\tilde{\alpha}_m^{(n,l)} = 0$, which means that these two modes are (elliptically) polarized in the plane perpendicular to **B**. Furthermore,

$$\tilde{\alpha}_n^{(n,l)} = \left(\omega_m^2 - \Omega^{(n,l)2}\right)\left(\omega_l^2 - \Omega^{(n,l)2}\right) + i\Omega^{(n,l)}\omega_{\rm B}\varepsilon_{nml} \times \left(\omega_m^2 - \Omega^{(n,l)2}\right) \propto \frac{\omega_l^2 - \Omega^{(n,l)2}}{\Omega^{(n,l)}\omega_{\rm B}} + i\varepsilon_{nml}\,,$$
$$\tilde{\alpha}_l^{(n,l)} \propto \frac{\omega_n^2 - \Omega^{(n,l)2}}{\Omega^{(n,l)}\omega_{\rm B}} + i\varepsilon_{lmn}\,, \tag{38}$$

where a choice of an upper index on the left-hand side affects only upper indices on the right-hand side, and the same is true for lower indices.

Let us specialize further to the case of small $k$, for which the frequencies have been given in Sec. III. If $m = 3$, the first magnetized mode (cyclotron) is circularly polarized with

$$\boldsymbol{\alpha}^{(1)} = \frac{1}{2\sqrt{\omega_{\rm B}}}[(1+i)\mathbf{e}_1 + (1-i)\mathbf{e}_2]. \tag{39}$$

The second magnetized mode (soft quadratic) is elliptically polarized with

$$\boldsymbol{\alpha}^{(2)} = \sqrt{\frac{c_1c_2}{2\omega_{\rm B}(c_1^2+c_2^2)}}\left[\left(\frac{c_2}{c_1} - i\right)\mathbf{e}_1 + \left(\frac{c_1}{c_2} + i\right)\mathbf{e}_2\right], \tag{40}$$

which becomes circular for $c_1 = c_2$.

If $m = 1$ and there is no electron polarization, then

$$\tilde{\alpha}_2^{(2)} \propto \left(\frac{\omega_{\rm p}}{c_2k}\right)\frac{\sqrt{1+b^2}}{b} - i,\ \tilde{\alpha}_3^{(2)} \propto \left(\frac{c_2k}{\omega_{\rm p}}\right)\frac{b}{\sqrt{1+b^2}} + i \approx i, \tag{41}$$

on account of $c_2k \ll \omega_{\rm p}$ (although to get normalization right, one has to keep the imaginary term in the expression for $\tilde{\alpha}_2^{(2)}$). The normalized coefficient for the second magnetized mode (acoustic with suppressed sound speed) thus reads

$$\boldsymbol{\alpha}^{(2)} = \frac{b\sqrt{c_2k}}{\sqrt{2}\omega_{\rm p}(1+b^2)^{3/4}}\left[\frac{\omega_{\rm p}\sqrt{1+b^2}}{c_2kb}\,\mathbf{e}_2 + i(\mathbf{e}_3 - \mathbf{e}_2)\right] \approx \frac{\mathbf{e}_2}{(1+b^2)^{1/4}\sqrt{2c_2k}}, \tag{42}$$

which means that this mode is essentially linearly polarized. The third mode (optic with the hybrid frequency) is elliptically polarized with the normalized coefficient

$$\boldsymbol{\alpha}^{(3)} = \frac{b}{(1+b^2)^{1/4}\sqrt{2\omega_{\rm p}(1+2b^2)}} \times \left[\left(\frac{b}{\sqrt{1+b^2}} + i\right)\mathbf{e}_2 + \left(\frac{\sqrt{1+b^2}}{b} - i\right)\mathbf{e}_3\right]. \tag{43}$$

For $b \gg 1$, the polarization of this mode becomes circular.

If $m = 2$, then normalized $\alpha$-coefficients are obtained from the expressions for the $m = 1$ case by complex conjugation followed by replacements $c_2 \to c_1$ and $\mathbf{e}_2 \to \mathbf{e}_1$.

Finally, if electrons are polarizable, nothing changes for the $m = 3$ case, but there are slight changes for $m = 1$ and 2. Since the frequency of the converted mode, $\sqrt{\xi}\omega_{\rm p}$, is still much bigger than the acoustic frequencies, $c_{1,2}k$, the only thing that occurs is that $\omega_{\rm p}$ gets replaced by $\sqrt{\xi}\omega_{\rm p}$ in the above formulae. Hence, if $m = 1$

$$\boldsymbol{\alpha}^{(2)} = \frac{b\sqrt{c_2k}}{\sqrt{2}\omega_{\rm p}\xi^{1/4}(\xi+b^2)^{3/4}} \times \left[\left(\frac{\sqrt{\xi}\omega_{\rm p}}{c_2k}\right)\frac{\sqrt{\xi+b^2}}{b}\,\mathbf{e}_2 + i(\mathbf{e}_3 - \mathbf{e}_2)\right] \approx \frac{\xi^{1/4}\mathbf{e}_2}{(\xi+b^2)^{1/4}\sqrt{2c_2k}},$$
$$\boldsymbol{\alpha}^{(3)} = \frac{b}{(\xi+b^2)^{1/4}\sqrt{2\omega_{\rm p}(\xi+2b^2)}} \times \left[\left(\frac{b}{\sqrt{\xi+b^2}} + i\right)\mathbf{e}_2 + \left(\frac{\sqrt{\xi+b^2}}{b} - i\right)\mathbf{e}_3\right]. \tag{44}$$

The same transformation as in the rigid background case yields normalized $\alpha$-coefficient in the $m = 2$ case.

## VI. A NOTE ON THE PHONON SPECTRUM OF THE HCP LATTICE

One can easily generalize Eq. (17) for crystals with more than one ion in the primitive cell. The dynamic matrix for such a Coulomb crystal with a polarizable electron background is presented in Appendix. One of the most well-known examples is the hexagonal close-packed (hcp) lattice. The properties of an hcp Coulomb crystal with a rigid electron background without and with a magnetic field were analyzed previously.[18–20] The spectrum of the hcp lattice consists of six modes [solid black curves in Fig. 2(a)]. Three of them (which we shall call "standard modes") are similar to the modes of the bcc lattice, namely, two modes are acoustic and the third one is optic $\approx\omega_{\rm p}$. In the absence of the magnetic field, the two acoustic modes of the hcp lattice cross each other in some directions of the wavevector **k** [as seen in Fig. 2(a)], which never occurs in the bcc lattice. The other three modes (which we shall call "basis modes") are optic and correspond to oscillations of ions inside the primitive cell with respect to each other.

The behavior of the standard modes for a polarizable electron background and in a magnetic field coincides with the behavior of the respective modes of the bcc lattice. In particular, in a non-magnetized crystal, the electron background polarizability affects only the standard optic mode by converting it into an acoustic one. Basis and acoustic modes do not change. This is illustrated in Fig. 2(a) by (red) dots for $g = 0.05$ and by (blue) dashes for $g = 0.5$.

In a magnetized crystal with a rigid background for orthogonal propagation [Fig. 2(b)], one of the standard acoustic modes is not affected, the other one decreases as $(1+b^2)^{-1/2}$, and the standard optic mode grows as $\sqrt{1+b^2}$. For parallel propagation [Fig. 2(c)], the standard modes produce a cyclotron mode $\approx\omega_{\rm B}$, a soft mode $\propto k^2/b$, and an

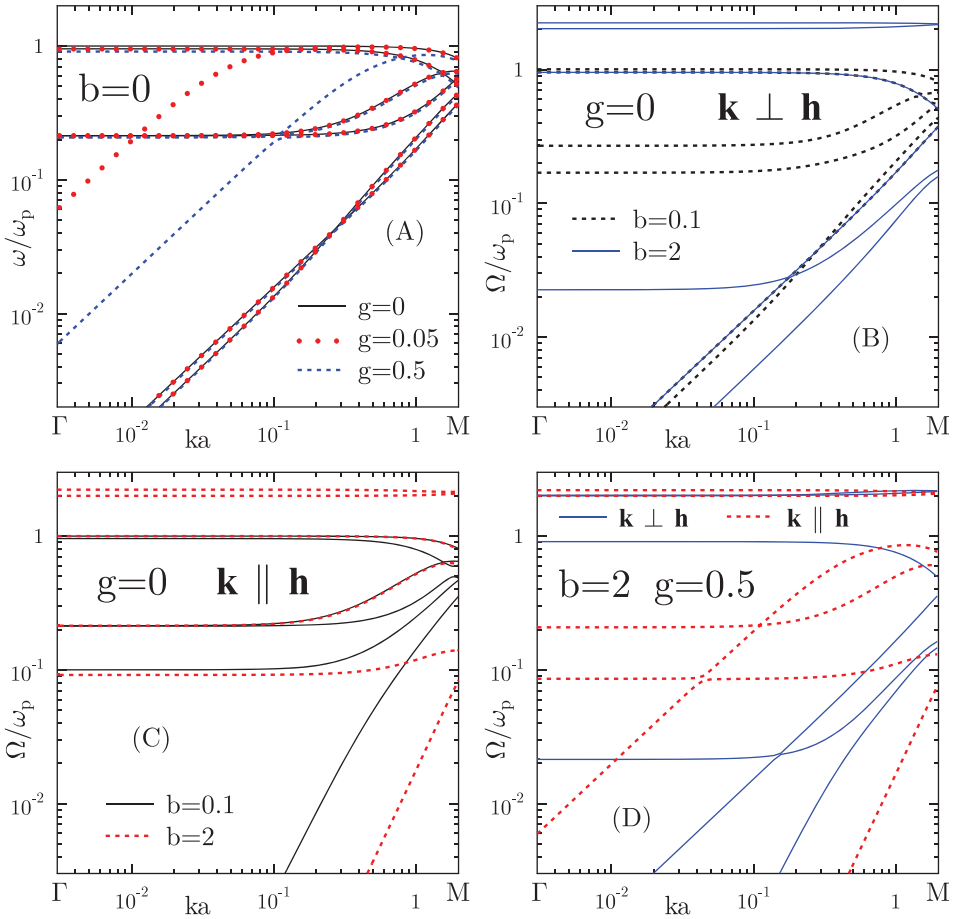


FIG. 2. Dispersion curves of the hcp lattice for different $b$, $g$, and $\mathbf{h}$. The Cartesian coordinate system is directed so that the edge $\Gamma M$ lies on the axis $k_x$. In panel B, $\mathbf{h} = (0, 0, 1)$, and in panel C, $\mathbf{h} = (1, 0, 0)$.

optic mode insensitive to the field $\approx\omega_p$. This reproduces our analysis in Sec. III for the modes of the bcc lattice.

The basis modes of a magnetized crystal remain optic [cf. Figs. 2(b) and 2(c)]. One of them is insensitive to the magnetic field, another one grows for $b > 1$ approximately $\propto b$ and is very close to the upper standard (cyclotron) mode, and the third one decreases approximately as $1/b$ (also for $b > 1$). Qualitatively, these tendencies can be understood if one switches temporarily to the bcc lattice. This lattice can be treated (artificially) as a simple cubic lattice with two ions in the primitive cell, six phonon modes at each $\mathbf{k}$, and a two times smaller Brillouin zone (see Ref. 21 for details). Then, of the six modes at a given $\mathbf{k} = (k_x, k_y, k_z)$, three modes coincide with the standard bcc lattice modes at this $\mathbf{k}$, while the other three coincide with the standard modes of the bcc lattice at $\tilde{\mathbf{k}} = (2\pi/a_l - k_x, k_y, k_z)$. This (reflected) $\tilde{\mathbf{k}}$ belongs to the bcc lattice Brillouin zone but does not belong to the smaller simple cubic lattice Brillouin zone. Thus, the latter three modes are a continuation of the former three (standard) modes. Returning to the case of the hcp lattice, we can effectively view the basis mode as a "continuation" of the standard ones across the "reflection" point M. This is further corroborated by an observation that the six solid (blue) curves in Fig. 2(b) can be split into three pairs with very close frequencies at M. The same is true for dashed (red) curves in Fig. 2(c). Consequently, it appears natural that the basis modes demonstrate the same general trends with $b$ as their respective standard modes.

In Fig. 2(d), we show modes propagating parallel (red, dashed) and orthogonal (blue, solid) to the field for $b = 2$ and $g = 0.5$. If $\mathbf{k} \perp \mathbf{h}$, only the lower standard acoustic mode is sensitive to the polarization as it acquires a soft quadratic segment at $k < \kappa_{TF}$. If $\mathbf{k} \parallel \mathbf{h}$, the standard optic mode $\approx\omega_p$ is converted into an acoustic one, while the other standard modes remain intact. The same effects have been seen in Sec. III. Basis modes in a magnetized hcp crystal are virtually unaffected by the electron polarization.

## VII. CONCLUSION

We have studied phonon modes and polarization vectors of Coulomb crystals of ions in the presence of a uniform magnetic field taking the polarizability of the electron background into account.

The phonon spectrum of crystals with one ion in the primitive cell (e.g., the bcc lattice) consists of three modes. For $k \gg \kappa_{TF}$, electron polarizability is not important, and all modes have the same frequencies as in the Coulomb crystal with a rigid electron background. At $k \ll \kappa_{TF}$, the background compressibility has a pronounced effect. One of the modes is linear ($\Omega \propto k$). If $\mathbf{k} \cdot \mathbf{h} = 0$, its frequency is independent of $b$ and $\kappa_{TF}$. For parallel propagation, its frequency is $\propto 1/\kappa_{TF}$. Another mode is quadratic ($\Omega \propto k^2$). Its frequency is $\propto 1/(b\kappa_{TF})$ for $\mathbf{k} \cdot \mathbf{h} = 0$, but it is $\propto 1/b$ for $\mathbf{k} \parallel \mathbf{h}$. The third mode is optic with frequency $\approx\omega_B$ for any propagation angle.

For crystals with two ions in the primitive cell (e.g., the hcp lattice), in addition to three similar modes, there exist three other modes, which are optic and are practically unaffected by the background polarization. For any other crystals, the phonon spectrum with background polarization can be calculated using a general expression for the Coulomb crystal dynamic matrix supplied in Appendix.

We have presented a detailed analysis of polarization vectors of phonon modes of a magnetized bcc crystal with or without electron screening. The most transparent formulae were obtained in the cases where the magnetic field was directed along one of the polarization vectors of a non-magnetized crystal.

These results can be used for realistic calculations of electron-phonon scattering rates and electron thermal and electrical conductivities in neutron star crust.

## ACKNOWLEDGMENTS

This work was supported by Russian Science Foundation Grant No. 14-12-00316.

## APPENDIX: THE DYNAMIC MATRIX FORMULA

The dynamic matrix for a Coulomb crystal with $N_{\rm cell} > 1$ ions in the primitive cell and polarizable electron background reads

$$
\begin{aligned}
D_{\mu p,\nu p'}(\mathbf{k})\frac{M}{Z^2e^2} = \frac{4\pi n}{N_{\rm cell}}\Bigg\{ & \sum_{\mathbf{G}} \frac{(G_\mu+k_\mu)(G_\nu+k_\nu)}{(\mathbf{G}+\mathbf{k})^2+\kappa_{\rm TF}^2}\exp\left[-\frac{(\mathbf{G}+\mathbf{k})^2+\kappa_{\rm TF}^2}{4A^2}+i(\mathbf{G}+\mathbf{k})(\boldsymbol{\chi}_p-\boldsymbol{\chi}_{p'})\right] \\
& - \delta_{pp'}\sum_{\mathbf{G}p''}\frac{G_\mu G_\nu}{G^2+\kappa_{\rm TF}^2}\exp\left[-\frac{G^2+\kappa_{\rm TF}^2}{4A^2}+i\mathbf{G}(\boldsymbol{\chi}_p-\boldsymbol{\chi}_{p''})\right]\Bigg\} - \sum_{\mathbf{R}}{}'\Bigg\{\left(\frac{\delta_{\mu\nu}}{Y_{p'}^3}-\frac{3Y_{p'\mu}Y_{p'\nu}}{Y_{p'}^5}\right) \\
& \times\left[(\kappa_{\rm TF}Y_{p'}-1)E_{p'}^{+}-(\kappa_{\rm TF}Y_{p'}+1)E_{p'}^{-}-\frac{4AY_{p'}}{\sqrt{\pi}}F_{p'}\right]+\frac{Y_{p'\mu}Y_{p'\nu}}{Y_{p'}^2}\left(\kappa_{\rm TF}^2E_{p'}^{+}+\kappa_{\rm TF}^2E_{p'}^{-}-\frac{8A^3Y_{p'}}{\sqrt{\pi}}F_{p'}\right)\Bigg\}e^{i\mathbf{k}\cdot\mathbf{R}} \\
& + \delta_{pp'}\sum_{\mathbf{R}p''}{}'\Bigg\{\left(\frac{\delta_{\mu\nu}}{Y_{p''}^3}-\frac{3Y_{p''\mu}Y_{p''\nu}}{Y_{p''}^5}\right)\left[(\kappa_{\rm TF}Y_{p''}-1)E_{p''}^{+}-(\kappa_{\rm TF}Y_{p''}+1)E_{p''}^{-}-\frac{4AY_{p''}}{\sqrt{\pi}}F_{p''}\right] \\
& + \frac{Y_{p''\mu}Y_{p''\nu}}{Y_{p''}^2}\left(\kappa_{\rm TF}^2E_{p''}^{+}+\kappa_{\rm TF}^2E_{p''}^{-}-\frac{8A^3Y_{p''}}{\sqrt{\pi}}F_{p''}\right)\Bigg\}, \qquad \text{(A1)}
\end{aligned}
$$

$p,p',p''=1,\ldots,N_{\rm cell}$ enumerate ions in the primitive cell, $\boldsymbol{\chi}_p$ are respective basis vectors ($\boldsymbol{\chi}_1=0$),

$$
\begin{aligned}
E_{p',p''}^{\pm} &= e^{\pm\kappa_{\rm TF}R}\,\mathrm{erfc}\left(AY_{p',p''}\pm\kappa_{\rm TF}/(2A)\right), \\
F_{p',p''} &= \exp\left(-\frac{\kappa_{\rm TF}^2}{4A^2}-A^2Y_{p',p''}^2\right), \qquad \text{(A2)}
\end{aligned}
$$

$\mathbf{Y}_{p',p''}=\mathbf{R}+\boldsymbol{\chi}_p-\boldsymbol{\chi}_{p',p''}$, prime at sums means that terms with $Y_{p'}=0$ and $Y_{p''}=0$ should be omitted, $A$ is an arbitrary parameter chosen so that sums over direct and reciprocal lattice vectors, and $\mathbf{R}$ and $\mathbf{G}$, converge equally rapidly (e.g., $A=1/a$).


[1]H. E. DeWitt, W. L. Slattery, and J. Yang, Phys. Nonideal Plasmas **26**, 11 (1992).
[2]A. Kanaan, A. Nitta, D. E. Winget, S. O. Kepler, M. H. Montgomery, T. S. Metcalfe, H. Oliveira, L. Fraga, A. F. M. da Costa, J. E. S. Costa, B. G. Castanheira, O. Giovannini, R. E. Nather, A. Mukadam, S. D. Kawaler, M. S. O'Brien, M. D. Reed, S. J. Kleinman, J. L. Provencal, T. K. Watson, D. Kilkenny, D. J. Sullivan, T. Sullivan, B. Shobbrook, X. J. Jiang, B. N. Ashoka, S. Seetha, E. Leibowitz, P. Ibbetson, H. Mendelson, E. G. Meistas, R. Kalytis, D. Alisauskas, D. O'Donoghue, D. Buckley, P. Martinez, F. van Wyk, R. Stobie, F. Marang, L. van Zyl, W. Ogloza, J. Krzesinski, S. Zola, P. Moskalik, M. Breger, A. Stankov, R. Silvotti, A. Piccioni, G. Vauclair, N. Dolez, M. Chevreton, J. Deetjen, S. Dreizler, S. Schuh, J. M. Gonzalez Perez, R. Østensen, A. Ulla, M. Manteiga, O. Suarez, M. R. Burleigh, and M. A. Barstow, Astron. Astrophys. **432**, 219 (2005).
[3]M. H. Cohen and F. Keffer, Phys. Rev. **99**, 1128 (1955).
[4]W. J. Carr, Jr., Phys. Rev. **122**, 1437 (1961).
[5]E. L. Pollock and J. P. Hansen, Phys. Rev. A **8**, 3110 (1973).
[6]N. A. Usov, Y. B. Grebenschikov, and F. R. Ulinich, J. Exp. Theor. Phys. **51**, 148 (1980).
[7]D. A. Baiko, J. Phys.: Conf. Ser. **496**, 012010 (2014).
[8]D. A. Baiko, Mon. Not. R. Astron. Soc. **458**, 2840 (2016).
[9]G. I. Svetozarova and V. N. Tsytovich, Izv. Vuzov Radiofiz. **5**, 658 (1962).
[10]L. Hernquist, Astrophys. J. Suppl. Ser. **56**, 325 (1984).
[11]D. G. Yakovlev and D. A. Shalybkov, Sov. Sci. Rev., Ser. E: Astrophys. Space Phys. **7**, 311 (1989).
[12]W. B. Hubbard and W. L. Slattery, Astrophys. J. **168**, 131 (1971).
[13]D. A. Baiko, Phys. Rev. E **66**, 056405 (2002).
[14]D. A. Baiko, Phys. Rev. E **80**, 046405 (2009).
[15]For brevity, we suppress index **k** at frequencies and polarization vectors of the phonon modes till the end of the section.
[16]In this section lower index **k** has to be restored because it is important to distinguish quantities with indices **k** and –**k**.
[17]From now on we can again drop the index **k**; non-normalized α-coefficients are labelled by a tilde, and the normalized ones are not.
[18]T. Nagai and H. Fukuyama, J. Phys. Soc. Jpn. **52**, 44 (1983).
[19]A. A. Kozhberov and D. A. Baiko, Astrophys. Space Sci. **359**, 50 (2015).
[20]A. A. Kozhberov, Astrophys. Space Sci. **361**, 256 (2016).
[21]A. A. Kozhberov and D. A. Baiko, Contrib. Plasma Phys. **52**, 153 (2012).